Interaction between long-crested random waves and a submerged horizontal cylinder

Felice Arena[a)]
Department of Mechanics and Materials, "Mediterranea" University of Reggio Calabria, Loc. Feo di Vito, 89100 Reggio Calabria, Italy

(Received 31 October 2005; accepted 9 May 2006; published online 14 July 2006)

This paper is concerned with the interaction between long-crested random waves and a submerged horizontal cylinder in deep water. The analytical linear predictions are obtained by extending the classical linear solution for the diffraction of monochromatic waves by a horizontal submerged cylinder, to the random waves by applying the theory of wind-generated waves. It is obtained that the wave pressure, which represents a random Gaussian process, has an amplitude that increases on the upper half-cylinder and decreases on the lower half-cylinder, with respect to the wave pressure amplitude at the same depth in an undisturbed wave field. The random wave force is derived by integration of the wave pressure on the cylinder. Both the horizontal and the vertical force components have equal standard deviation and very narrow spectra. By applying the quasideterminism theory, is then obtained that both the wave pressure and the wave force on the cylinder, when a very high wave occurs, are quasi-impulsive in the time domain. Finally, the analytical predictions are compared with the data of a small-scale field experiment. It is shown that the linear theory well predicts the drop of the propagation speed of the wave pressure on the cylinder. Some discrepancies have been noted for the standard deviation of the random wave force, which is overestimated by analytical predictions. © *2006 American Institute of Physics*.
[DOI: 10.1063/1.2213867]

I. INTRODUCTION

The problem of the interaction between gravity waves and a submerged horizontal circular cylinder in deep water was first treated by Dean,[1] who proved that, according to the linear theory, the surface waves suffer a phase shift in passing over the cylinder. He also obtained the remarkable result that, to the first order, there is no reflected wave from the cylinder.

Ogilvie,[2] following Ursell's earlier paper,[3] obtained the linear velocity potential and the oscillatory force. Arena[4] found that the velocity potential in Ogilvie's paper lacks an additional time periodic term, constant in space, that modifies the wave pressure but has no influence on the wave force.

McIver and McIver[5] and Palm[6] obtained analytically that there is no reflected wave to the second order either. These theoretical results agree well with the experimental evidence by Chaplin,[7] which showed that the reflection is negligible either to the second or to the third order. Chaplin[7] also obtained that the oscillatory force on the submerged horizontal cylinder may be as much as 50% less than the linear theory prediction.

In this paper, according to the two-dimensional theory of wind-generated waves (Longuet-Higgins[8] and Phillips[9]), the analytical linear solution is obtained for the interaction between long-crested random waves and a submerged horizontal cylinder in deep water. The random wave pressure on the surface of the submerged circular cylinder is first compared with the wave pressure at the same depth in the undisturbed field.

The random wave force on the submerged horizontal circular cylinder is then obtained by pressure integration on the cylinder. In particular the standard deviation of the wave force is obtained as a function of the standard deviation of the surface displacement in an undisturbed wave field. Both the horizontal and the vertical force components are random Gaussian processes, to the first order in a Stokes expansion. Furthermore they have very narrow spectra, as was pointed out first by Boccotti[10,11] with experimental evidence and recently by Arena[12] who investigated the statistical properties of the random wave force and obtained the theoretical spectrum of the force process.

Time histories of wave pressure and of wave force on the cylinder, when a very high wave occurs on it, are obtained by applying the quasideterminism theory (Boccotti[11,13] and Boccotti *et al.*[14]). This theory enables us to predict the wave force components and the wave pressure on the cylinder when either an exceptionally high wave occurs over the cylinder or an extremely large force occurs. In particular the drop of the propagation speed of the wave pressure on the cylinder is analyzed. A physical interpretation for this phenomenon was suggested by Ogilvie,[2] which is satisfactory for a large value of the cylinder radius. Recently by experimental evidence Boccotti[11] found a reduction of about 50% of the propagation speed of the pressure head waves at a few horizontal submerged cylinders in the field, and he suggested a physical interpretation based on a linear inviscid pattern holding whatever the cylinder radius.

[a)]Telephone: +39 (0)965 875 292. Fax: +39 (0)965 875 201. Electronic mail: arena@unirc.it

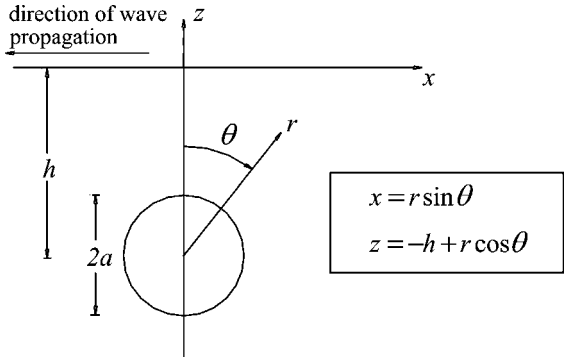

FIG. 1. Reference sketch.

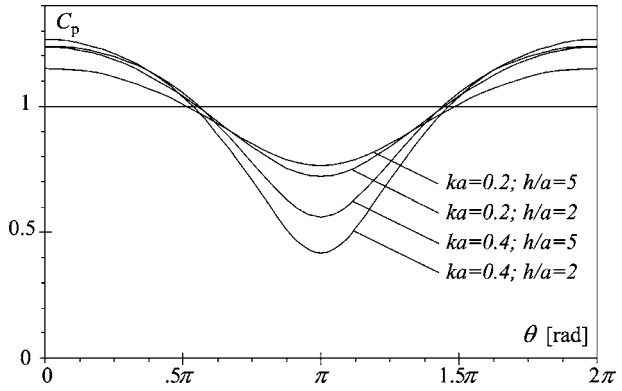

FIG. 2. The diffraction coefficient C_p on a submerged horizontal cylinder for fixed values of the radius ($ka=0.2$ and $ka=0.4$) and of the submergence of the cylinder center ($h/a=2$ and $h/a=5$). The mean JONSWAP spectrum has been assumed.

The theoretical predictions are finally compared with the results of a small-scale field experiment (Boccotti[10,11] and Arena[12]).

II. LONG-CRESTED RANDOM WAVES ON A SUBMERGED HORIZONTAL CYLINDER

The horizontal circular cylinder, of radius a, is submerged beneath waves in an infinite depth and has its center at point $x=0$, $z=-h$ (see Fig. 1). The incident random wave train travels in the direction opposite to the x axis. The wave crests are parallel to the axis of the cylinder. The motion is assumed irrotational with inviscid and incompressible fluid.

Following the general theory of wind-generated waves, we define a random sea state as the sum of an infinitely large number N of periodic waves having small amplitude α_j and angular frequencies ω_j different from each other. The random phase angles ζ_j are uniformly distributed over the range $0<\zeta_j<2\pi$. Both the wave elevation and the velocity potential, with the above-mentioned hypotheses, represent a random stationary Gaussian process of time.

Let the potential of the incident waves in a random two-dimensional sea state be the real part of

$$\phi_i(r,\theta,t) = g\sum_{j=1}^{N} \alpha_j \omega_j^{-1} \exp(-k_j h)\exp[k_j r \exp(-\mathrm{i}\theta)] \times \exp[-\mathrm{i}(\omega_j t+\zeta_j)], \tag{1}$$

where g is the gravitational acceleration, t is the time, and $k_j=\omega_j^2/g$ is the wave number. The surface displacement is then

$$\eta_i(x,t) = \sum_{j=1}^{N} \alpha_j \sin(k_j x+\omega_j t+\zeta_j) \tag{2}$$

and its variance

$$\sigma^2 = \int_0^\infty E(\omega)d\omega, \tag{3}$$

where $E(\omega)$ is the frequency spectrum of the surface displacement in an undisturbed field, defined as

$$E(\omega) = \frac{1}{2}\sum_j \alpha_j^2 \quad \text{for } j \text{ such that} \quad \omega<\omega_j<\omega+d\omega. \tag{4}$$

The total velocity potential ϕ is obtained adding the velocity potential of the scattered wave to the one of the incident wave ϕ_i [Eq. (1)]. It is given by

$$\phi(r,\theta,t) = g\sum_{j=1}^{N} \alpha_j \omega_j^{-1} e^{-k_j h}[-P(r,\theta,\omega_j)\sin(\omega_j t+\zeta_j) + Q(r,\theta,\omega_j)\cos(\omega_j t+\zeta_j)], \tag{5}$$

where

$$P(r,\theta;\omega) = \frac{1}{1+S_\varepsilon^2}\left\{\sum_{n=1}^{\infty}\varepsilon_n D_n[\sin(n\theta)-S_\varepsilon\cos(n\theta)] + \sum_{n=1}^{\infty} n\varepsilon_n(S_\varepsilon A_n - B_n)\right\}, \tag{6}$$

$$Q(r,\theta;\omega) = 1+\frac{1}{1+S_\varepsilon^2}\left\{\sum_{n=1}^{\infty}\varepsilon_n D_n[\cos(n\theta)+S_\varepsilon\sin(n\theta)] - \sum_{n=1}^{\infty} n\varepsilon_n(A_n+S_\varepsilon B_n)\right\}, \tag{7}$$

being $\varepsilon_n(ka,kh)$ $(n=1,\ 2,\ 3,\ \ldots)$ the solutions of the infinite set of equations

$$\varepsilon_n + (ka)^{2n}\sum_{m=1}^{\infty}\frac{(n+m)!}{n!(m-1)!}A_{n+m}\varepsilon_m = \frac{(ka)^{2n}}{n!}. \tag{8}$$

Functions A_n, B_n, D_n, and S_ε are defined, respectively, as

$$A_n(kh) = \frac{1}{n(2kh)^n} + \frac{2}{n!}\left[\exp(-2kh)\mathrm{P}\int_{-\infty}^{2kh}\frac{\exp u}{u}\mathrm{d}u - \sum_{m=1}^{n}\frac{(m-1)!}{(2kh)^m}\right], \quad n\geqslant 1, \tag{9}$$

$$B_n(kh) = \frac{2\pi\exp(-2kh)}{n!}, \tag{10}$$

$$D_n(kr,ka) = \frac{1}{(kr)^n} + \frac{(kr)^n}{(ka)^{2n}}, \tag{11}$$

$$S_\varepsilon(ka,kh) = 2\pi \exp(-2kh) \sum_{n=1}^{\infty} \frac{\varepsilon_n}{(n-1)!}, \tag{12}$$

where the symbol P denotes the principal value of the integral.

The diffraction coefficient C_p of the wave pressure

The wave pressure is obtained from Bernoulli equation

$$\Delta p = -\rho \frac{\partial \phi}{\partial t}, \tag{13}$$

and its variance $[\sigma_p^2 \equiv <\Delta p^2(r,\theta,t)>]$ is given by

$$\sigma_p^2 = (\rho g)^2 \int_0^\infty E(\omega)\exp(-2kh)[P^2(r,\theta,\omega) + Q^2(r,\theta,\omega)]d\omega. \tag{14}$$

We define the diffraction coefficient C_p of the wave pressure, the ratio of the standard deviation of the wave pressure at a fixed point (r,θ), to the standard deviation of the wave pressure $\Delta p_i[\equiv -\rho(\partial\phi_i/\partial t)]$ at the same depth $(z=-h+r\cos\theta)$ in an undisturbed wave field. From the definition it follows that

$$C_p(r,\theta) = \sqrt{\frac{\int_0^\infty E(\omega)\exp(-2kh)[P^2(r,\theta,\omega) + Q^2(r,\theta,\omega)]d\omega}{\int_0^\infty E(\omega)\exp(-2kh)\exp(2kr\cos\theta)d\omega}}. \tag{15}$$

Figure 2 shows the diffraction coefficient (15) on a submerged horizontal cylinder for fixed values of the radius and of the submergence of cylinder center. The mean JONSWAP spectrum (Hasselmann *et al.*[15]) has been assumed. As we may see the wave pressure increases (with respect to the wave pressure at the same depth in an undisturbed wave field) on the upper half-cylinder and decreases on the lower half-cylinder. The maximum diffraction coefficient $C_{p_{\max}}$ is at the top of the cylinder $(\theta=0)$, the minimum $C_{p_{\min}}$ is at the cylinder bottom $(\theta=\pi)$.

Let us note that, for a fixed value of h/a, the diffraction effects increase as the radius ka increases. The diffraction effects decrease as kh increases, for a fixed value of ka.

We have also that $C_{p_{\max}}$ is slightly affected by spetral bandwidth; its value decreases as the spectrum gets narrower.

III. THE RANDOM WAVE FORCE

The linear wave force on the cylinder (per unit length) is obtained by integrating the pressure fluctuations Δp on the solid cylinder. Its components are

$$F_x(t) = -2\pi\rho g \sum_{j=1}^{N} \alpha_j k_j^{-1} \exp(-k_j h)\varepsilon_{1j}(1+S_{\varepsilon j}^2)^{-1/2} \times \cos(\omega_j t - \varphi_j + \zeta_j), \tag{16}$$

$$F_z(t) = -2\pi\rho g \sum_{j=1}^{N} \alpha_j k_j^{-1} \exp(-k_j h)\varepsilon_{1j}(1+S_{\varepsilon j}^2)^{-1/2} \times \sin(\omega_j t - \varphi_j + \zeta_j), \tag{17}$$

where

$$\varphi_j = \arctan(S_{\varepsilon j}). \tag{18}$$

The horizontal and vertical force components have equal standard deviation, that is given by

$$\sigma_F = 2\pi\rho g \sqrt{\int_0^\infty E(\omega)k^{-2}\exp(-2kh)\varepsilon_1^2(1+S_\varepsilon^2)^{-1}d\omega}, \tag{19}$$

where $E(\omega)$ is the frequency spectrum of the incident waves [Eq. (4)].

It is convenient to define dimensionless coefficient

$$f = \frac{\sigma_F}{2\pi\rho g^2 \omega_p^{-2}\sigma}, \tag{20}$$

where σ and ω_p are, respectively, the standard deviation of the surface displacement and the peak frequency of the incident waves. This coefficient is given by

$$f = \sqrt{\int_0^\infty E(\omega)(\omega/\omega_p)^{-4} \exp(-2kh)\varepsilon_1^2(1+S_\varepsilon^2)^{-1}\mathrm{d}\omega \Big/ \int_0^\infty E(\omega)\mathrm{d}\omega}, \tag{21}$$

and is shown in Fig. 3 as a function of ka, for fixed values of h/a.

IV. THE TIME HISTORIES OF WAVE PRESSURES AND WAVE FORCES ON THE CYLINDER WHEN EITHER A VERY HIGH WAVE, OR A VERY LARGE FORCE, OCCURS

The quasideterminism theory (Boccotti[11,13] and Boccotti *et al.*[14]) enables us to foretell what happens when a very large wave height occurs at a fixed point in a random wave field (very large wave height with respect to the mean wave height at this point). The theory, which is derived analytically, may be applied either for waves in an undisturbed field or for waves in a nonhomogeneous field.

In this paper the quasideterminism theory is applied in two different forms, either to foretell what happens when a very large height of the wave pressure occurs at a fixed point (r,θ) on or near the cylinder at a fixed instant t_o (see Sec. IV A) or to foretell what happens when a very large wave force occurs on the cylinder at a fixed instant t_o (see Sec. IV B).

Let us note that we may apply the quasideterminism theory to the wave force process directly, the wave force being a stationary Gaussian random process of time.

The instant t_o when the high wave occurs is conventionally defined as the instant in which the crest of the highest wave occurs at the fixed point.

A. What happens if a very high wave occurs over the cylinder

If a wave of the pressure fluctuation with a given crest-to-trough height H occurs at a fixed point (r_o,θ_o) and H is very large with respect to the mean wave height at this point, we may expect the pressure fluctuation η_{ph} $[\equiv \Delta p/(\rho g)]$ to be very close to the deterministic form

$$\begin{aligned}\eta_{ph}(r_o+\Delta r,\theta_o+\Delta\theta,t_o+T) &= \frac{H}{2}[\langle \eta_{ph}(r_o,\theta_o,t)\,\eta_{ph}(r_o+\Delta r,\theta_o+\Delta\theta,t+T)\rangle \\ &\quad - \langle \eta_{ph}(r_o,\theta_o,t)\,\eta_{ph}(r_o+\Delta r,\theta_o+\Delta\theta,t+T-T^*)\rangle]/ \\ &\quad [\langle \eta_{ph}^2(r_o,\theta_o,t)\rangle - \langle \eta_{ph}(r_o,\theta_o,t)\,\eta_{ph}(r_o,\theta_o,t+T^*)\rangle];\end{aligned} \tag{22}$$

and we may expect the force components F_x and F_z to be very close to the deterministic form

$$F_x(t_o+T) = \frac{H}{2}\frac{\langle \eta_{ph}(r_o,\theta_o,t)F_x(t+T)\rangle - \langle \eta_{ph}(r_o,\theta_o,t)F_x(t+T-T^*)\rangle}{\langle \eta_{ph}^2(r_o,\theta_o,t)\rangle - \langle \eta_{ph}(r_o,\theta_o,t)\,\eta_{ph}(r_o,\theta_o,t+T^*)\rangle}; \tag{23}$$

$$F_z(t_o+T) = \frac{H}{2}\frac{\langle \eta_{ph}(r_o,\theta_o,t)F_z(t+T)\rangle - \langle \eta_{ph}(r_o,\theta_o,t)F_z(t+T-T^*)\rangle}{\langle \eta_{ph}^2(r_o,\theta_o,t)\rangle - \langle \eta_{ph}(r_o,\theta_o,t)\,\eta_{ph}(r_o,\theta_o,t+T^*)\rangle}; \tag{24}$$

where T^* is the abscissa of the absolute minimum of the autocovariance function of the wave pressure, defined as

$$\psi(T) \equiv \langle \eta_{ph}(r_o,\theta_o,t)\,\eta_{ph}(r_o,\theta_o,t+T)\rangle. \tag{25}$$

Equations (22)–(24) may be rewritten as functions of the frequency spectrum $E(\omega)$ of surface incident waves. We obtain, respectively,

$$\begin{aligned}\eta_{ph}(r_o+\Delta r,\theta_o+\Delta\theta,t_o+T) &= \frac{H}{2}\int_0^\infty E(\omega)e^{-2kh}\{[P_1P_2+Q_1Q_2] \\ &\quad \times[\cos(\omega T)-\cos(\omega(T-T^*))]+[P_1Q_2-P_2Q_1] \\ &\quad \times[\sin(\omega T)-\sin(\omega(T-T^*))]\}d\omega \Big/ \\ &\quad \int_0^\infty E(\omega)e^{-2kh}[P_1^2+Q_1^2][1-\cos(\omega T^*)]d\omega;\end{aligned} \tag{26}$$

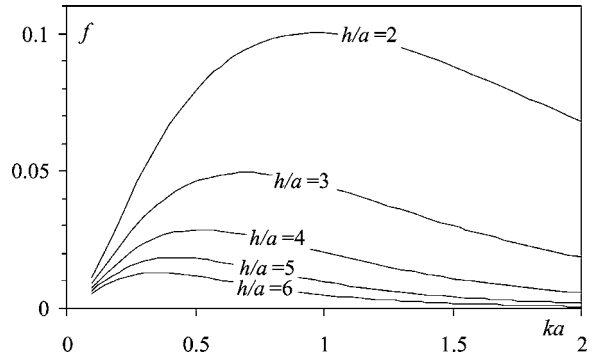

FIG. 3. The dimensionless coefficient f [Eq. (21)] as a function of ka for fixed values of the submergence of cylinder center h/a. The mean JONSWAP spectrum has been assumed.

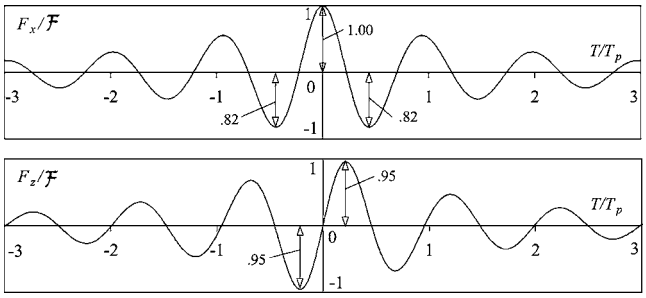

FIG. 4. What happens when a positive peak $\mathcal{F}$ of the horizontal force F_x on the cylinder occurs (the peak occurs at time instant $T=0$): the time histories of the force components F_x and F_z for $ka=0.2$ and $kh=0.6$. The mean JONSWAP spectrum has been assumed for the surface displacement.

$$F_x(t_o+T) = -2\pi\rho g\frac{H}{2}\int_0^\infty E(\omega)k^{-1} \times\exp(-2kh)\frac{\varepsilon_1}{\sqrt{1+S_\varepsilon^2}}\{P_1[\cos(\omega T) - \cos(\omega(T-T^*))] - Q_1[\sin(\omega T) - \sin(\omega(T-T^*))]\}d\omega \Big/ \int_0^\infty E(\omega)\exp(-2kh)[P_1^2+Q_1^2][1-\cos(\omega T^*)]d\omega; \tag{27}$$

$$F_z(t_o+T) = -2\pi\rho g\frac{H}{2}\int_0^\infty E(\omega)k^{-1} \times\exp(-2kh)\frac{\varepsilon_1}{\sqrt{1+S_\varepsilon^2}}\{P_1[\sin(\omega T) - \sin(\omega(T-T^*))] + Q_1[\cos(\omega T) - \cos(\omega(T-T^*))]\}d\omega \Big/ \int_0^\infty E(\omega)\exp(-2kh)[P_1^2+Q_1^2][1-\cos(\omega T^*)]d\omega, \tag{28}$$

where

$$P_1 \equiv P(r_o,\theta_o,\omega); \quad Q_1 \equiv Q(r_o,\theta_o,\omega); \quad P_2 \equiv P(r_o+\Delta r,\theta_o+\Delta\theta,\omega); \quad Q_2 \equiv Q(r_o+\Delta r,\theta_o+\Delta\theta,\omega). \tag{29}$$

B. What happens if a very large force occurs on the cylinder

If a very large wave force (very large with respect to the mean wave force) with an amplitude of $\mathcal{F}$ occurs on the cylinder at the time t_o, we can foresee the force components in the time domain. Specifically, if at a time t_o a very large value $\mathcal{F}$ (positive or negative) of the horizontal force F_x occurs, we may expect the force components to be very close to the deterministic form:

$$F_x(t_o+T) = \mathcal{F}\frac{\langle F_x(t)F_x(t+T)\rangle}{\langle F_x^2(t)\rangle}, \tag{30}$$

$$F_z(t_o+T) = \mathcal{F}\frac{\langle F_x(t)F_z(t+T)\rangle}{\langle F_x^2(t)\rangle}, \tag{31}$$

and, as function of $E(\omega)$:

$$F_x(t_o+T) = \mathcal{F}\frac{\int_0^\infty E(\omega)k^{-2}\exp(-2kh)\frac{\varepsilon_1^2}{1+S_\varepsilon^2}\cos(\omega T)d\omega}{\int_0^\infty E(\omega)k^{-2}\exp(-2kh)\frac{\varepsilon_1^2}{1+S_\varepsilon^2}d\omega}, \tag{32}$$

$$F_z(t_o+T) = \mathcal{F}\frac{\int_0^\infty E(\omega)k^{-2}\exp(-2kh)\frac{\varepsilon_1^2}{1+S_\varepsilon^2}\sin(\omega T)d\omega}{\int_0^\infty E(\omega)k^{-2}\exp(-2kh)\frac{\varepsilon_1^2}{1+S_\varepsilon^2}d\omega}. \tag{33}$$

Figure 4 shows the time histories of the force components F_x and F_z when a positive peak $\mathcal{F}$ of F_x occurs on a cylinder ($ka=0.2$, $kh=0.6$ and the mean JONSWAP spectrum have been assumed).

As we can see the random wave force is quasi-impulsive in the time domain (let us recall that the wave force is sinusoidal in the time domain for monochromatic waves). We have also that both the positive peak $F_{z_{\max}}$ and the negative peak $F_{z_{\min}}$ (in absolute value) of the vertical force are slightly smaller than $\mathcal{F}$ (value of the positive peak of F_x). The absolute values of negative peaks $F_{x_{\min}}$ are 18% smaller than the maximum F_x. These differences are a bandwidth effect, and indeed they increase as the bandwidth increases. As an example with the Pierson-Moskowitz spectrum (Pierson and Moskowitz[16]), which has a bandwidth greater than the JONSWAP spectrum, the absolute value of $F_{x_{\min}}$ proves to be 21% smaller than the maximum of F_x.

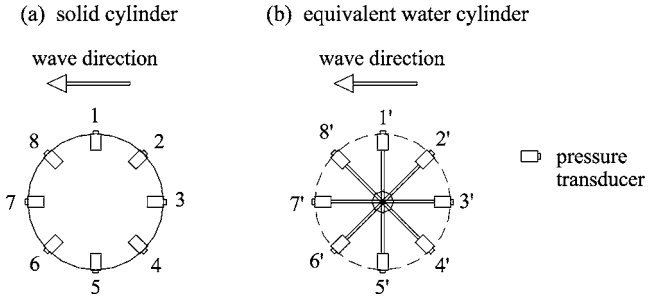

FIG. 5. Experiment gauges: the 16 pressure transducers assembled on the median vertical section of the solid cylinder (transducers 1–8) and on the radiant crown (transducers $1'-8'$).

Let us note that with a similar procedure, we can foresee the force components when a very large value $\mathcal{F}$ (positive or negative) of the vertical force F_z occurs on the cylinder.

V. COMPARISON WITH THE DATA OF A SMALL-SCALE FIELD EXPERIMENT

The small-scale field experiment was carried out off the beach of Reggio Calabria (eastern coast of the Strait of Messina). Standard deviation of the surface displacements in an undisturbed field was between 0.05 m and 0.1 m, and peak period was between 1.8 s and 2.6 s.

At first a cylinder and a radiant crown were assembled. The cylinder had radius a of 0.45 m, length of 4 m, and submergence h of its center between 1.35 m (low tide) and 1.55 m (high tide). The radiant crown, in an undisturbed wave field, had equal radius, equal submergence and equal position of the solid cylinder. Afterwards a cylinder and a radiant crown with $a=0.225$ m and h between 1.125 m and 1.325 m were assembled.

The mean water depth was between 2.9 m (low tide) and 3.1 m (high tide). Eight transducers, assembled on the cylinders [see Fig. 5(a)], measured the pressure fluctuations on the median vertical section of the cylinder. From these transducers we estimate the wave force on the median section.

Eight transducers, assembled on the vertical radiant crown [see Fig. 5(b)], measured the pressure fluctuations on the water-equivalent cylinder.

Three ultrasonic wave probes measured the surface wave elevation over the cylinder and in an undisturbed wave field.

During the experiment 581 records (381 with the 0.45 m cylinder and 200 with the 0.225 m cylinder) were collected. Each record had duration of 540 s, with a sampling rate of 10 Hz for each gauge (see Boccotti[11] for more details).

In this paper only pure wind wave records (without overlapping swells) with dominant direction perpendicular to the cylinder axis have been analyzed.

A. The diffraction coefficient C_p of the wave pressure

Figure 6 shows the diffraction coefficients C_p measured in three records. As we can see the theoretical C_p overestimate the data, but confirm two experimental results: the C_p is greater than 1 in the upper half-cylinder and is smaller than 1 in the lower half-cylinder; the values of C_p for $\theta=\pi/2$ (transducer 3) and $\theta=3/2\pi$ (transducer 7) are close to 1.

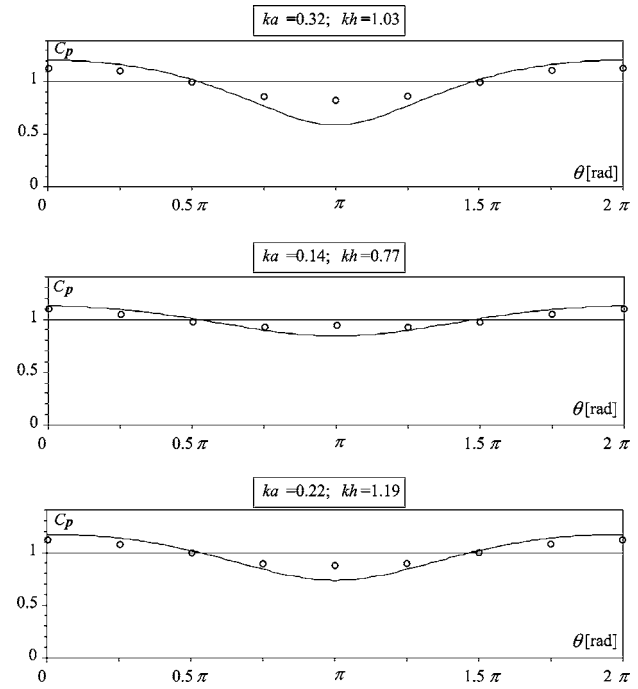

FIG. 6. The diffraction coefficient C_p of the wave pressure, on the cylinder surface. The continuous lines represent the theoretical distribution from Eq. (12) with experimental values of ka and kh (frequency spectrum is the mean JONSWAP).

B. The wave force components

1. The measured force

The experimental wave force on the cylinder has been obtained from the wave pressures recorded by gauges 1–8 (see Fig. 5). In particular the wave force components for each instant have been calculated from the eight values of the wave pressure at that instant.

Figure 7 shows the experimental values of f_{F_z} vs f_{F_x} [f_{F_x} and f_{F_z} being coefficient (20) with σ_F being the standard deviation of, respectively, horizontal force F_x and vertical force F_z]: the left panel shows the data for the cylinder radius $a=0.45$ m; the right panel shows the data for $a=0.225$ m.

As we may see, for $a=0.45$ m the values of f_{F_x} and f_{F_z} are very close to each other, according to the linear theory prediction; the mean value of f_{F_x}/f_{F_z} is equal to 0.997.

Some differences have been obtained for the $a=0.225$ m cylinder, as we may also appreciate from Fig. 8, which shows the values of the quotient f_{F_x}/f_{F_z} (obtained from data) vs ka. We have that f_{F_x}/f_{F_z} values tend to de-

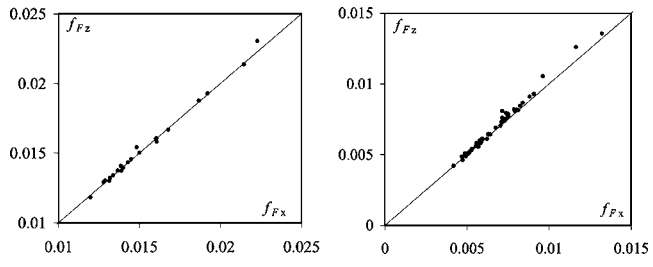

FIG. 7. The experimental values of f_{F_x} vs f_{F_z}. Left panel: $a=0.45$ m cylinder. Right panel: $a=0.225$ m cylinder.

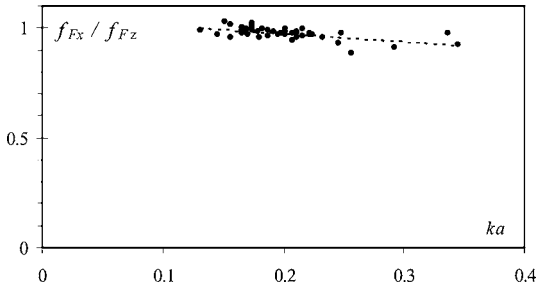

FIG. 8. The experimental values of f_{F_x}/f_{F_z} vs ka, for cylinder radius $a=0.225$ m. Dashed line gives the linear regression.

crease as ka increases. The linear regression (dashed line) is over the range (0.92, 1.0) in the experimental range of ka.

2. Comparison between measured force and analytical linear prediction

The experimental values of f_{F_x} and f_{F_z} have been compared with theoretical values of f obtained from Eq. (21). In particular predictions have been obtained from the experimental values of ka and kh, for a mean JONSWAP spectrum.

It is obtained that the experimental wave forces (and therefore both f_{F_x} and f_{F_z}) are smaller than the linear predictions.

Figure 9 shows, for the $a=0.45$ m cylinder, the values of the quotient between the standard deviation σ_{F_x} of the experimental horizontal force, and the standard deviation σ_F of the theoretical force, as a function of the Keulegan-Carpenter number K_C. As we can see, for K_C close to 2 experimental forces are as much as one half the analytical linear prediction, in full agreement with the experimental evidence by Chaplin.[7] We have also that the value of σ_{F_x}/σ_F decreases as K_C decreases. Note that Chaplin[7] (see also Grue[17]) analyzed the interaction between regular waves and a submerged horizontal circular cylinder, at low Keulegan-Carpenter numbers; he found that it is a strongly nonlinear phenomenon, which even fully nonlinear models are not able to predict. The most relevant result was the decay of the inertia coefficient to one half of theoretical inviscid value (equal to 2), for K_C close to 2.5. In this paper a further confirmation of his result has been found, for random sea waves. The nonlinear behavior of the force is due to the interaction between the steady streaming (viscous flow) attached to the cylinder and the incident orbital wavy flow. This interaction (Magnus effect) induces a force that is π out of phase with the inertial force.

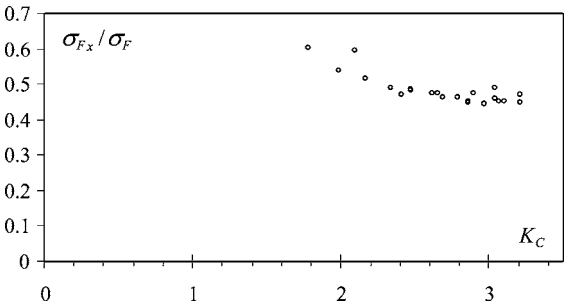

FIG. 9. The $a=0.45$ m cylinder. The values of the quotient between standard deviation σ_{F_x} of experimental horizontal force and standard deviation σ_F of theoretical force, as a function of the Keulegan-Carpenter number K_C.

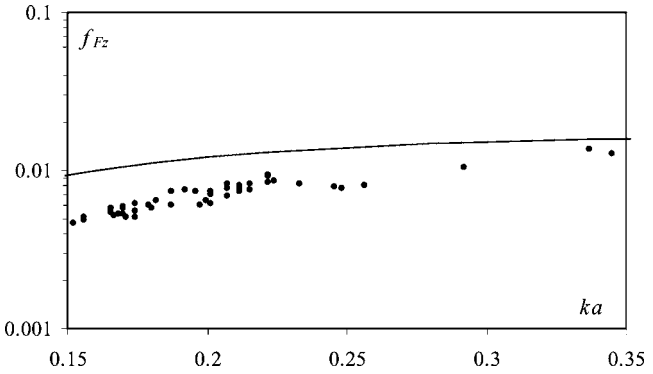

FIG. 10. Comparison between experimental values of f_{F_z} for the $a=0.225$ m cylinder, and analytical predictions (continuous line) obtained from Eq. (21) for a mean JONSWAP spectrum.

Finally Fig. 10 shows, for the $a=0.225$ m cylinder, the comparison between the analytical f obtained from Eq. (21), and the experimental values of f_{F_z}. As we can see values of f_{F_z}/f are over the range $0.50<f_{F_z}/f<0.75$.

C. Application of the quasideterminism theory

The quasideterminism theory may be directly applied from experimental data. Figure 11 shows the data of record 516 ($ka=0.19$ and $kh=1.03$); dotted lines show the pressure fluctuation at the transducers 1–8 and the wave force components, when a pressure head wave of a given very large height H occurs at point $(a,0)$ (transducer 1). They have been obtained by means of Eqs. (22)–(24). The time averages on the right-hand sides of these equations have been obtained directly from the time series data of a 9 min record including about 250 individual waves.

Continuous lines in Fig. 11 show theoretical predictions. Specifically they show the time histories of the pressure

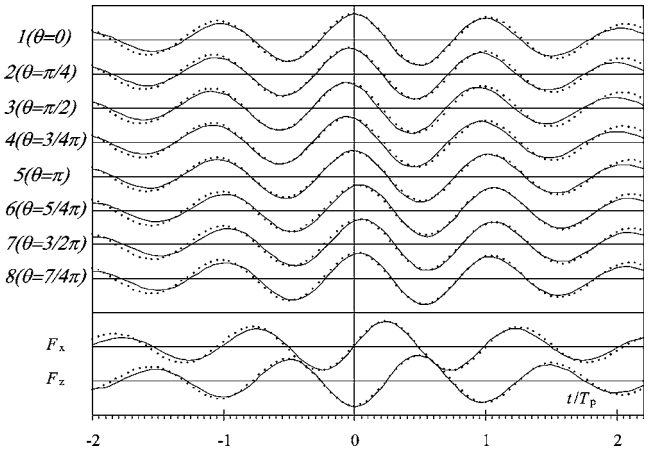

FIG. 11. Record No. 516 ($ka=0.19$ and $kh=1.03$). What happens when a very large height of the pressure fluctuation occurs at transducer 1 (see Fig. 5). Dotted lines are obtained from experimental data. Continuous lines show analytical predictions obtained from Eqs. (26)–(28), using experimental values of ka and kh; theoretical spectrum is the mean JONSWAP (all the time histories are normalized).

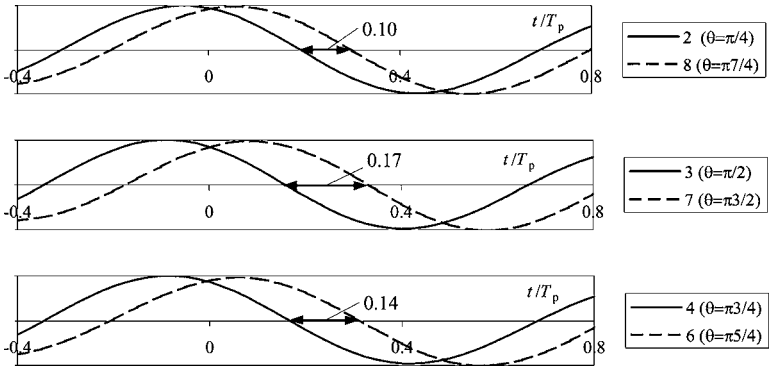

FIG. 12. The theoretical phase lags ε_{28}, ε_{37}, and ε_{46} on the solid cylinder, when a large pressure wave occurs at point $(a,0)$. Predictions are obtained from Eq. (26), for $ka=0.26$, and $h/a=3.2$; the mean JONSWAP spectrum has been assumed. Let us note that ε_{ij} gives the time that the wave pressure takes to pass from point i to point j (points i and j have equal submergence and are on the solid cylinder).

fluctuation [Eq. (26)] and of the wave force components [Eqs. (27) and (28)] when a pressure head wave of given very large height H occurs at point $(a,0)$. Experimental values of ka and kh and the mean JONSWAP spectrum have been assumed.

As we can see analytical predictions and data are very close indeed. In particular both theoretical predictions and data show that the pressure fluctuations suffer a phase shift in passing over the cylinder (see next section) and the pressure fluctuation at transducers 1 and 5 are in phase.

Let us note that, as a consequence of the finite bandwidth of the spectrum, pressure fluctuations and wave forces are quasi-impulsive in the time domain. Furthermore, we have a confirmation of the results of the previous section: the measured and calculated forces have equal periods and equal spectra (see Arena[12]). Therefore, the Magnus force, which produces the reduction of the force amplitude, does not modify the structure of force process in time domain.

1. The drop of the propagation speed of the wave pressure on the cylinder

The drop of the propagation speed of the wave pressure on a horizontal submerged cylinder was observed with experimental evidence by Boccotti.[11] He analyzed the phase shift between wave pressure at transducers 2 and 8, 3 and 7, 4 and 6 (see Fig. 5) and obtained that the pressure head wave takes a time to pass on the solid cylinder that is greater than on the equivalent water cylinder.

Specifically, by analyzing the records with the $a=0.45$ m cylinder, he found that the wave pressure takes a time ε_{28} to pass from point 2 to point 8 on the solid cylinder, that is near 1.7 times greater than the time $\varepsilon_{2'8'}$ to pass from point $2'$ to point $8'$ on the equivalent water cylinder (that is $\varepsilon_{28}/\varepsilon_{2'8'}\cong 1.7$). Furthermore with experimental evidence he found $\varepsilon_{37}/\varepsilon_{3'7'}\cong 2$ and $\varepsilon_{46}/\varepsilon_{4'6'}\cong 2.3$.

As for the records with the $a=0.225$ m cylinder he found that the reduction of the propagation speed was somewhat smaller.

The analytical predictions are obtained from Eq. (26). Figures 12 and 13 show the analytical predictions for $ka=0.26$, $h/a=3.2$, assuming the mean JONSWAP spectrum. In particular Fig. 12 shows the phase lags ε_{28}, ε_{37}, and ε_{46} on the solid cylinder, when a large pressure wave occurs at point 1 [having polar coordinates $(a,0)$]. Figure 13 shows the phase lags $\varepsilon_{2'8'}$, $\varepsilon_{3'7'}$, and $\varepsilon_{4'6'}$ on the equivalent water cylinder, when a very large wave pressure occurs at point $1'$. As we can see the linear theory well predicts the phase lag: theoretical $\varepsilon_{28}/\varepsilon_{2'8'}$, $\varepsilon_{37}/\varepsilon_{3'7'}$, and $\varepsilon_{46}/\varepsilon_{4'6'}$ are equal to 1.67, 1.89, and 2.33, respectively.

As for the smaller cylinder ($a=0.225$ m), by analytical prediction (see continuous lines in Fig. 11) we obtain $\varepsilon_{28}/\varepsilon_{2'8'}=1.73$, $\varepsilon_{37}/\varepsilon_{3'7'}=1.92$, and $\varepsilon_{46}/\varepsilon_{4'6'}=2.24$.

In conclusion analytical linear predictions, obtained from Eq. (26), agree well with the experimental evidence by Boccotti.

VI. CONCLUSIONS

The analytical linear solution for the interaction between two-dimensional wind-generated waves and a horizontal submerged cylinder has been obtained, extending classical Ogilvie's solution (Ref. 2; see also Arena[4]).

It has been obtained that wave pressure amplitude increases on the upper half-cylinder and decreases on the lower

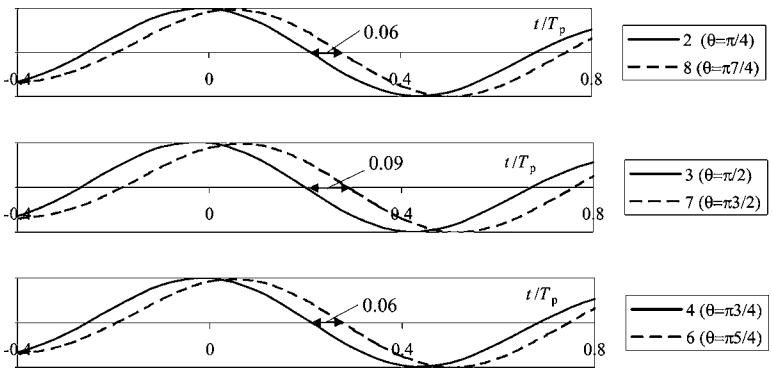

FIG. 13. The phase lags $\varepsilon_{2'8'}$, $\varepsilon_{3'7'}$ and $\varepsilon_{4'6'}$ on the equivalent water cylinder, when a large pressure wave occurs at point $(a,0)$ in an undisturbed wave field. Predictions are obtained for $ka=0.26$, and $h/a=3.2$; the mean JONSWAP spectrum has been assumed. Let us note that ε_{ij} gives the time that the wave pressure takes to pass from point i to point j (points i and j have equal submergence and are on the equivalent water cylinder).

half-cylinder. Furthermore the propagation speed of the wave pressure suffers a drop in passing on the cylinder. These analytical predictions well agree with experimental evidence by Boccotti,[11] who compared the cylinder force and the Froude-Krylov force and concluded that the vertical wave force on the solid cylinder is greater than the vertical wave force on the ideal water cylinder because the amplitude of the pressure fluctuations grows at the upper half-cylinder and decreases at the lower half-cylinder. As for the horizontal wave force on the submerged cylinder, he concluded that it is greater than horizontal force on the equivalent water cylinder as a consequence of the drop of the propagation speed.

Analytical predictions have shown also that wave force components, when either a high wave or a large force occurs, are quasi-impulsive in the time domain and have equal standard deviation, in good agreement with data of a small scale field experiment. Experimental forces are smaller than analytical predictions. For values of K_C close to 2, the standard deviation of measured force is as much as one half the analytical predictions, in agreement with experimental evidence by Chaplin.[7] This result is due to the interaction (Magnus force) of the steady streaming (viscous flow) at the cylinder with the incident orbital wavy flow, which produces a force out of phase of π, with respect to the inertial force.

[1] W. R. Dean, "On the reflection of surface waves by a submerged cylinder," Proc. Cambridge Philos. Soc. **44**, 483 (1948).
[2] T. F. Ogilvie, "First- and second-order forces on a cylinder submerged under a free surface," J. Fluid Mech. **16**, 451 (1963).
[3] F. Ursell, "Surface waves on deep water in the presence of a submerged circular cylinder," Proc. Cambridge Philos. Soc. **46**, 141 (1950).
[4] F. Arena, "Note on a paper by Ogilvie: the interaction between waves and a submerged horizontal cylinder," J. Fluid Mech. **394**, 355 (1999).
[5] M. Mclver and P. Mclver, "Second-order wave diffraction by a submerged circular cylinder," J. Fluid Mech. **219**, 519 (1990).
[6] E. Palm, "Nonlinear wave reflection from a submerged circular cylinder," J. Fluid Mech. **233**, 49 (1991).
[7] J. R. Chaplin, "Non-linear forces on a horizontal cylinder beneath waves," J. Fluid Mech. **147**, 449 (1984).
[8] M. S. Longuet-Higgins, "The effects of non-linearities on statistical distributions in the theory of sea waves," J. Fluid Mech. **17**, 459 (1963).
[9] O. M. Phillips, "The theory of wind-generated waves," Adv. Hydrosci. **4**, 119 (1967).
[10] P. Boccotti, "Inertial wave loads on horizontal cylinders: a field experiment," Ocean Eng. **23**, 629 (1996).
[11] P. Boccotti, *Wave Mechanics for Ocean Engineering* (Elsevier, New York, 2000).
[12] F. Arena, "Statistics of wave forces on large horizontal cylinders," Ocean Eng. **29**, 359 (2002).
[13] P. Boccotti, "On mechanics of irregular gravity waves," Atti Accad. Naz. Lincei, Mem., Cl. Sci. Fis., Mat. Nat., Sez. 1a **8**, 111 (1989).
[14] P. Boccotti, G. Barbaro, and L. Mannino, "A field experiment on the mechanics of irregular gravity waves," J. Fluid Mech. **252**, 173 (1993).
[15] K. Hasselmann, T. P. Barnett, E. Bouws, H. Carlson, D. E. Cartwright, K. Enke, J. A. Ewing, H. Gienapp, D. E. Hasselmann, P. Krusemann, A. Meerburg, P. Müller, D. J. Olbers, K. Richter, W. Sell, and H. Walden, "Measurements of wind wave growth and swell decay during the Joint North Sea Wave Project (JONSWAP)," Dtsch. Hydrogr. Z. **A8**, 1 (1973).
[16] W. J. Pierson and L. Moskowitz, "A proposed spectral form for fully developed waves based on the similarity theory of S. A. Kitaigorodskii," J. Geophys. Res. **69**, 5181 (1964).
[17] J. Grue, "Nonlinear water waves at a submerged obstacle or bottom topography," J. Fluid Mech. **244**, 455 (1992).